ACS APPLIED MATERIALS & INTERFACES

Research Article

www.acsami.org

Multifunctional Graphene Sensors for Magnetic and Hydrogen Detection

Le Huang, Zhiyong Zhang,* Zishen Li, Bingyan Chen, Xiaomeng Ma, Lijun Dong, and Lian-Mao Peng*

Key Laboratory for the Physics and Chemistry of Nanodevices and Department of Electronics, Peking University, Beijing 100871, China

Supporting Information

ABSTRACT: Multifunctional graphene magnetic/hydrogen sensors are constructed for the first time through a simple microfabrication process. The as-fabricated graphene sensor may act as excellent Hall magnetic detector, demonstrating small linearity error within 2% and high magnetic resolution up to 7 mG/Hz$^{0.5}$. Meanwhile the same graphene sensor is also demonstrated as high-performance hydrogen sensor with high gas response, excellent linearity, and great repeatability and selectivity. In particular, the graphene sensor exhibits high hydrogen response up to 32.5% when exposed to 1000 ppm hydrogen, outperforming most graphene-based hydrogen sensors. In addition the hydrogen-sensing mechanism of Pd-decorated graphene is systematically explored through investigating its transfer characteristics during gas detection. Our work demonstrates that graphene is a terrific material for multifunctional sensing, which may in principle reduce the complexity of manufacturing process, lower the number of sensors required in the sensing systems, and potentially derive new and more powerful functions.

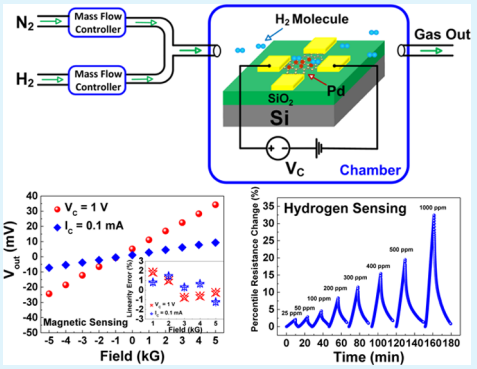

KEYWORDS: *graphene, multifunctional sensors, magnetic detection, hydrogen detection, Hall sensors*

1. INTRODUCTION

Electric sensors, which transfer external mechanical, magnetic, thermal, optical, or chemical stimuli to electrical signals, are routinely used everywhere, providing instrumentation for the monitoring of the state of the environment, security, supporting regulation of different processes, etc.[1] To provide more powerful electrical sensing systems, increasing types of sensors are required to provide comprehensive detection of external physical parameters, which inevitably increases the complexity of the systems. An efficient method to reduce the complexity without reducing functions is to adopt multifunctional sensors that can realize different functionalities with individual sensors. However, multifunctional sensors are seldom realized and used since it is a challenge to give consideration to different functions and to avoid the cross-talk among multifunctions.

Graphene is a promising material to construct high-performance electric sensors owing to its ultrathin body, high mobiltiy, maximum surface-to-volume ratio, high conductivity, low noise, and low defect density.[2−4] Since graphene is sensitive to magnetic field, gas, light, strain, and pressure, numerous sensors based on graphene channel have been demonstrated, including magnetic field sensors, gas sensors, optical sensors, pressure sensors, and biosensors.[5−18] In some favorable cases, graphene sensors have been shown to ourperform conventional sensors. For example graphene Hall elements (GHEs) for magnetic detection already outperform most conventional Hall sensors made from III−V compounds in many ways due to their high mobility, atomic thinness, and easy fabrication process.[5−12] Moreover profiting from the maximum surface-to-volume ratio and low noise, graphene is an ideal channel material for resistive gas/vapor sensors with high sensitivity and resolution.[13,14] Although many high-performance graphene sensors have been realized, all functions have already been realized using other semiconductors. In fact designing unique and irreplaceable sensors utilizing the unique properties of graphene is highly desirable to promote the applications of graphene sensors.

Here we reconsider the main properties of graphene on sensor applications and try to realize unique graphene sensors. Since graphene is sensitive to many kinds of stimulations, the main advantages of graphene-based sensors over conventional sensors are their multifunctionalities.[2] In other words, a single graphene device may in principle accomplish several sensing functions. Compared with fabricating several isolated sensors and integrating them together, the complexity of manufacturing a single multifunctional sensor is projected to be much lower.

In this work, multifunctional graphene sensors are first demonstrated for magnetic and hydrogen detection, which are two of the most widely used sensing tasks in practical applications. The fabrication processes are illustrated in Figure 1. Graphene sample is first transferred on SiO_2/Si substrate, which is then tailored into a cross-shaped channel and used to

Received: February 4, 2015
Accepted: April 22, 2015
Published: April 22, 2015

DOI: 10.1021/acsami.5b01070
ACS Appl. Mater. Interfaces 2015, 7, 9581−9588

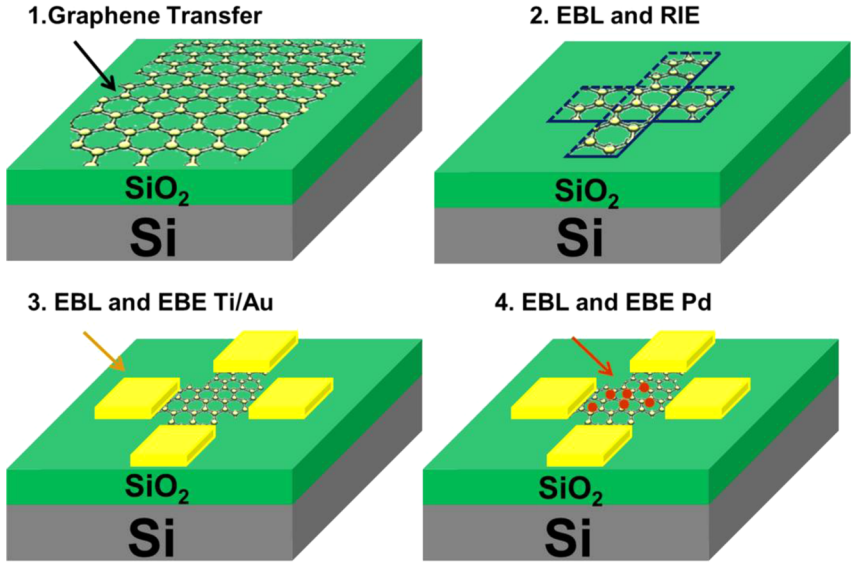

Figure 1. Fabrication process flow of the multifunctional graphene sensors. (1) The graphene is transferred onto the SiO_2/Si substrate by using a bubbling method, which is patterned by (2) electron beam lithography (BEL) and reactive ion etching (RIE). (3) Contacts to the graphene channel are fabricated using electron beam evaporation (EBE) and standard lift-off process. (4) The hydrogen-sensitive region is defined and fabricated by EBL and EBE of Pd particles.

construct Hall sensors. The graphene channel is then decorated using Pd nanoparticles to increase its sensitivity for hydrogen sensing. The as-fabricated graphene sensor exhibits high performance as Hall sensor, including excellent linearity and high resolution, and is also demonstrated as excellent hydrogen detector. The graphene sensor shows high hydrogen response ranging from 2.5% at 25 ppm to 32.5% at 1000 ppm hydrogen concentration owing to the very high carrier mobility in the graphene channel. The applications of multifunctional graphene sensors may in principle reduce the complexity of manufacturing process, lower the number of sensors required in the sensing systems, and potentially derive new and more powerful functions.

2. RESULTS AND DISCUSSION

As illustrated in Figure 1, the multifunctional graphene sensors were constructed through microfabrication process based on chemical vapor deposition (CVD)-derived graphene. Note that no additional processes were introduced into the fabrication procedure when compared with that of GHEs,[5,6,8,9] and the whole process is easy and compatible with silicon technology.[8] Figure 2a shows an optical image of a typical as-fabricated graphene sensor, in which the graphene channel was patterned into a cross-shape with a length-width ratio of 1.67 (100/60 μm). To make the device sensitive to hydrogen, the horizontal graphene channel is decorated with 1 nm thick Pd layer. The transfer characteristics shown in Figure 2b characterize the electric property of the graphene channel. The blue and red lines denote the transfer characteristics of the horizontal graphene channel before and after Pd decoration of the channel, respectively. It is clear that the pristine graphene channel demonstrates ambipolar conductivity with a Dirac point voltage of 8 V and on/off ratio of 10. On the contrary, Pd-decorated graphene exhibits monotonic and approximately linear transfer characteristic, and no exact Dirac point is observed within the gate voltage range used in this work. This is attributed to the heavy p-doping effect from Pd to the graphene channel, which significantly suppresses the electron conduction branch of the graphene channel.[19,20] The carrier mobility of the pristine graphene channel is extracted to be 5000 $cm^2/(V\ s)$ through peak transconductance method,[7] and the high quality of the pristine graphene is also verified by Raman spectrum (inset of Figure 2b) with a 2D/G peak ratio of 2.9. Obviously Pd decoration introduces extra carrier scattering and thus leads to degraded mobility, which is extracted to be 800 $cm^2/(V\ s)$. While Pd decoration significantly reduces the sensitivity of graphene Hall sensors, the sensors are still good ones, providing the necessary platform for constructing high-performance H_2 sensors.

Magnetic response of the multifunctional graphene sensor is first measured on a Hall probe station at room temperature and in air. A constant current or voltage bias was applied at the horizontal graphene channel, and an external magnetic field is applied normal to the sensor, which leads to a voltage between the vertical electrodes due to Hall effect. Before the decoration of Pd, the magnetic field-dependent Hall voltages in current (I_C = 0.1 mA) and voltage (V_C = 1 V) modes are presented in Figure 2c, in which Hall voltage increases linearly with magnetic field in both current (blue) and voltage (red) mode. In current mode the absolute sensitivity (S_A) of the graphene Hall sensor is 0.05 V/T, and the current-related sensitivity (S_I) is 500 V/AT. The corresponding carrier density is derived to be $1.25 \times 10^{12}/cm^2$. In voltage mode S_A is 0.17 V/T, and voltage-related sensitivity (S_V) is calculated to be 0.17/T. The corresponding Hall mobility is 2833 $cm^2/(V\ s)$. The inset of Figure 2c shows that the linearity error of the graphene Hall sensor is within 4% in current mode while within 12% in voltage mode from 1 to 5 kG. After Pd was deposited onto the horizontal graphene channel (marked in Figure 2a with blue dash line), the magnetic response results are plotted in Figure 2d. The Hall voltage of the graphene sensor increases with magnetic field in both current and voltage modes with small linearity error of less than 2% as shown in the inset of Figure 2d. However, the sensitivity of the graphene Hall sensor declines significantly with S_A of 0.17 V/T in current mode and 0.06 V/T in voltage mode. In this case, S_I and S_V decrease to 170 V/AT and 0.06/T,

DOI: 10.1021/acsami.5b01070
ACS Appl. Mater. Interfaces 2015, 7, 9581−9588

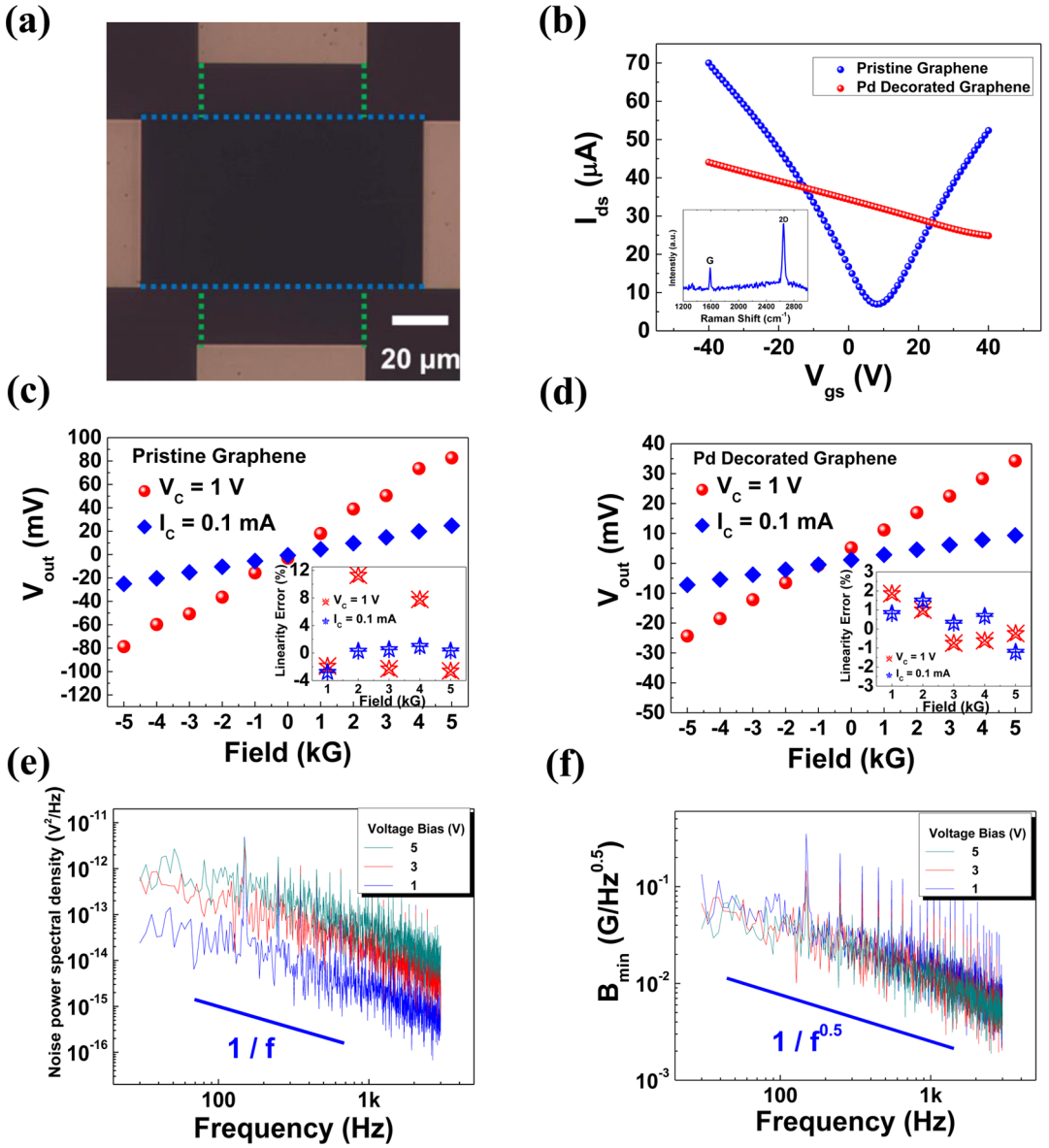

Figure 2. Characterization of the graphene sensors for magnetic detection at room temperature. (a) Optical image of the completed sensors. The dot lines denote the boundaries of graphene channel. The horizontal channel surrounded by blue dot line is covered by 1 nm Pd nanoparticles, while the rest of the channel is pristine graphene. (b) Transfer curves of the horizontal graphene channel before and after Pd decoration. The gate voltage is applied at the silicon substrate. (inset) Raman spectrum of pristine graphene channel with an excitation laser wavelength of 633 nm. (c) Magnetic response of the graphene sensors working under constant current and voltage excitation before Pd decoration. (inset) The linearity error of pristine graphene Hall sensors. (d) Magnetic response of the graphene sensors after Pd decoration. (inset) The linearity error of Pd-decorated graphene Hall sensors. (e) Low-frequency noise power spectral density and (f) magnetic resolution of the Pd-decorated graphene Hall sensors. The blue, red, and green lines are obtained with voltage biases of 1, 3, and 5 V, respectively.

respectively, which are about one-third compared with those of the pristine graphene based Hall sensor. The significant degradation on sensitivity after depositing Pd film is originated from the additional charge carrier density and scatterings induced by Pd decoration, since the carrier density n_{2D} and Hall mobility are 3.67×10^{12}/cm^2 and 1000 cm^2/(V s), respectively. However, the degraded S_I and S_V of the Pd-decorated graphene Hall sensor are still comparable with those of typical silicon-based Hall sensors, that is, 100 V/AT and 0.07/T.[21] In fact the main performance metrics including sensitivity and linearity of the graphene Hall sensors are strongly dependent on the definition of Pd-decorated region (Figure S1, Supporting Information), and the structure we used here is an optimized one. In addition, we studied the effect of the thickness of Pd layer to the performance of sensors. We deposited 1 nm Pd additionally on Pd-decorated graphene channel, which means that the graphene sensor was decorated by 2 nm Pd totally (Figure S2, Supporting Information). The results show that increasing Pd thickness leads to a slight increase in H_2 sensitivity but a severe decline in magnetic sensitivity. In other words, the 1 nm Pd we used in this work is also an optimal value.

Magnetic resolution B_{min} is another key parameter to benchmark the measuring accuracy of Hall sensors, and is determined by the ratio of electric noise voltage (N_V) and sensitivity S_A,[5,9] that is

$$B_{min} = N_V/S_A = P_V^{0.5}/S_A \quad (1)$$

DOI: 10.1021/acsami.5b01070
ACS Appl. Mater. Interfaces 2015, 7, 9581−9588

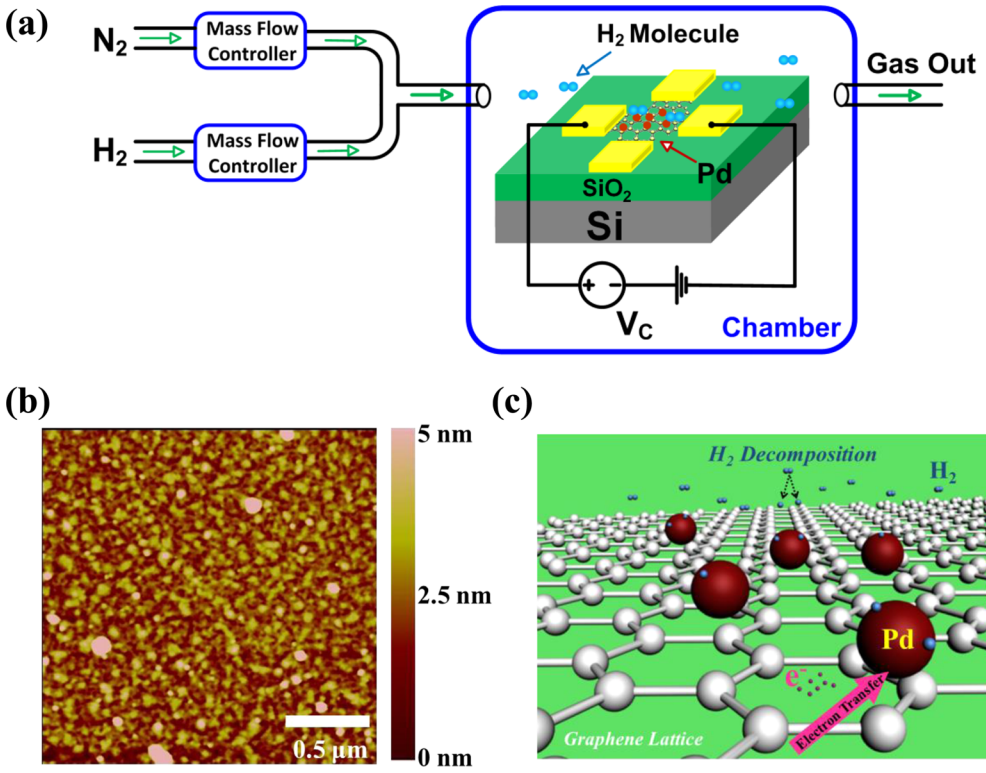

Figure 3. Multifunctional graphene sensors for H_2 detection. (a) Gas detection schematics of the graphene sensors. (b) Atomic-force-microscopic image of graphene channel covered with Pd nanoparticles. (c) Schematic diagram of interaction between graphene and Pd nanoparticles.

where P_v is the noise power spectral density of the graphene Hall sensor. P_v versus frequency f of the Pd-decorated graphene Hall sensors is measured through schematic of Figure S3 in Supporting Information, and the results are shown in Figure 2e. It is found that the noise follows a clear $1/f$ trend from 30 to 3 kHz, which testifies that flicker noise is the dominant noise source of our graphene devices at low frequency. The corresponding B_{min} of the Hall sensor is derived according to eq 1 and plotted in Figure 2f, showing clearly a $1/f^{0.5}$ trend but no dependence on bias voltage, and decreasing from 70 mG/Hz$^{0.5}$at 30 Hz to 7 mG/Hz$^{0.5}$ at 3 kHz. Note that such a high-resolution B_{min} is on the same order of magnitude with the best Hall sensors made from 2DEG, III−V compounds, and graphene.[5,9] Therefore, the Pd-decorated graphene Hall sensor discussed above is still among high-performance Hall sensors even after sacrificing performance for detecting hydrogen.

Since hydrogen is flammable and explosive, safety is vital in nearly all applications of hydrogen technology, for example, fuel cell, hydrogen storage, scientific research, and industrial production. At present, the most widely used hydrogen sensors are made from metal oxide, which requires high-temperature process (usually above 500 °C) and additional signal collection circuits.[22,23] Previous works have proven that pristine graphene is not sensitive to hydrogen[19,24] and thus cannot be used for fabricating hydrogen sensors directly. Nevertheless, the situation becomes different when Pd decoration is introduced. Pd nanoparticles are effective catalysts of hydrogen molecular adsorption and dissociation.[25,26] Various nano materials, such as graphene,[19,20,27] carbon nanotube,[28] nanowire,[29] and graphene network,[30] have been successfully fabricated into hydrogen sensors with the assist of Pd nanoparticles. Pd exhibits high sensitivity and selectivity in hydrogen sensing,[28−30] so it is also employed here as our hydrogen detection catalytic.

The horizontal graphene channel decorated with Pd nanoparticles (shown in Figure 2a) was used to perform the hydrogen sensing test, and the sensor was wire-bonded to a printed circuit board (PCB) and placed into a gas chamber (Figure S4, Supporting Information). Figure 3a illustrates the schematic of the hydrogen sensing test, and the two-terminal dynamic resistance of the graphene device was measured as a resistive gas sensor. To ensure the existence of Pd particles, the horizontal channel of the graphene device was measured through atomic force microscopy (AFM) as shown in Figure 3b. The Pd particles in the graphene-based hydrogen sensor as shown in Figure 3c are expected to perform two main functions. On the one hand, Pd particles accept electrons from graphene and lead to p-type doping of the graphene channel owing to the higher work function of Pd than that of graphene. On the other hand, Pd particles can act as an efficient catalytic for decomposing and adsorbing H_2 at graphene surface.

Gas response (GR) of a gas sensor is defined as the percentile resistance change when the sensor is exposed to the targeted gas,[19,20] that is

$$GR = (R_t - R_0)/R_0 \times 100\% \quad (2)$$

where R_t is the real-time resistance and R_0 is the initial resistance of the sensor at time $t = 0$. We first consider the effect of Pd particles in hydrogen sensing. Figure 4a contrasts the dynamic gas response of the graphene sensor before and after Pd decoration. The sensors were exposed to 750 sccm pure nitrogen for 10 min before the test to stabilize the initial resistance of the sensors. At time A, the sensors were exposed to 500 ppm hydrogen. After 10 min, hydrogen was shut off at time B, and the sensors recovered spontaneously in air. The

DOI: 10.1021/acsami.5b01070
ACS Appl. Mater. Interfaces 2015, 7, 9581−9588

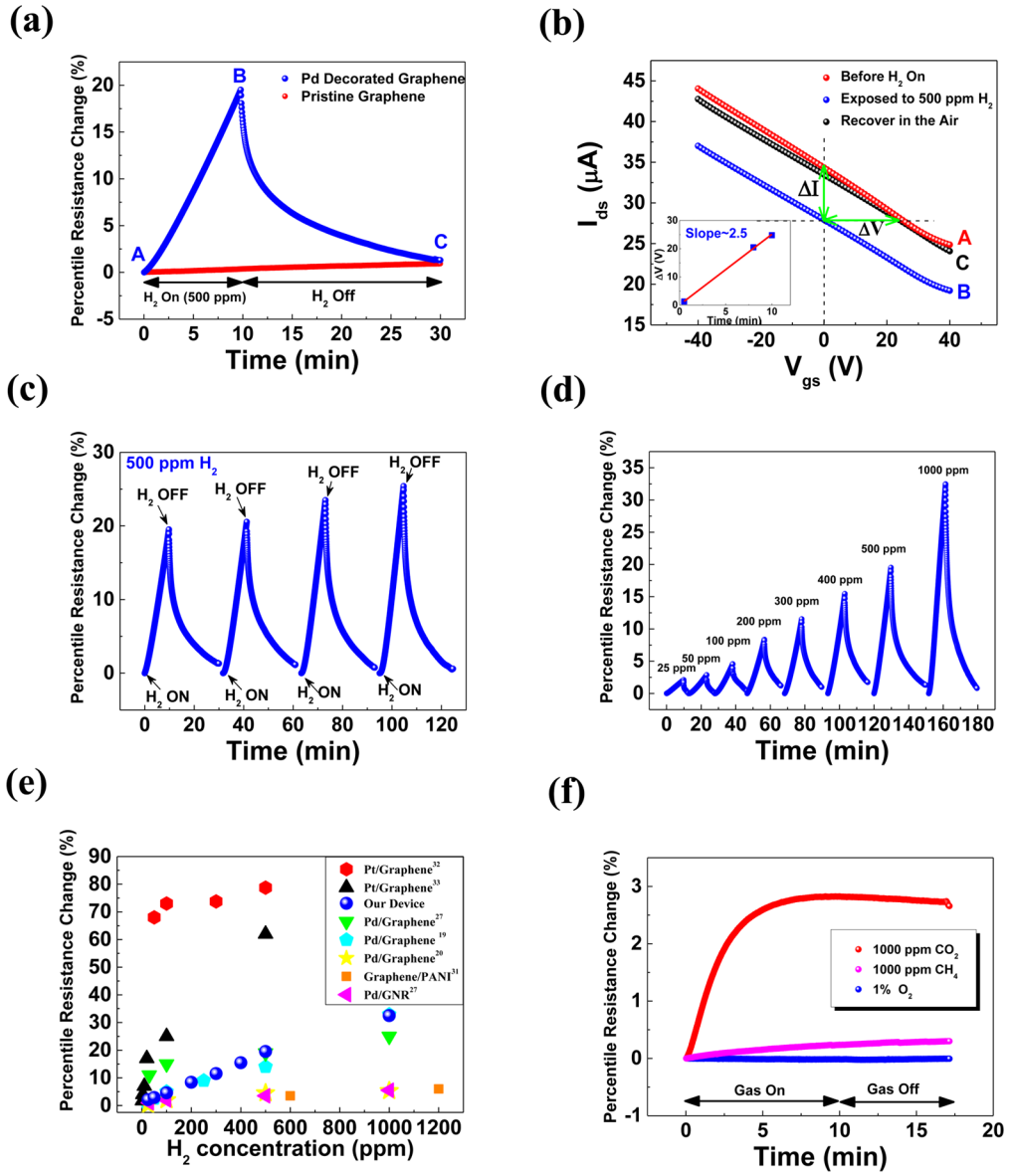

Figure 4. Characterization of the graphene sensors for gas detection. (a) Dynamic percentile resistance change before and after Pd decoration. The sensor is exposed to 500 ppm hydrogen for 10 min and then recovered in the air for 20 min. (b) Transfer characteristics of graphene sensors measured at three points in time A, B, and C in (a). The inset shows time-dependent ΔV during hydrogen sensing. (c) Repeatability test of graphene hydrogen sensors during four cycles of 500 ppm hydrogen on and off. (d) Dynamic percentile resistance change of the graphene sensors when exposed to hydrogen from 25 to 1000 ppm. (e) Gas response comparison of several graphene-based hydrogen sensors within similar hydrogen concentration range. (f) Selectivity test of the graphene hydrogen sensors when exposed to 1000 ppm carbon dioxide (CO_2), 1000 ppm methane (CH_4), and 1% oxygen (O_2).

pristine graphene-based device demonstrates weak response within 1% toward hydrogen. This is because hydrogen atoms only show little adsorption to pristine graphene.[24] By contrast, the resistance of the Pd-decorated graphene sensor increases greatly and follows an approximately linear relationship with time, reaching a gas response of 19.5% after 10 min. After hydrogen is shut off at time B, it takes about 20 min for the sensors to basically recover to the initial resistance at time C. This comparative test confirms that Pd nanoparticles sitting on the graphene channel play a decisive role in hydrogen sensing. It is well-known that some electrons in the graphene channel are transferred to Pd nanoparticles on graphene owing to the work function difference between Pd and graphene. When hydrogen is introduced into the chamber, some hydrogen molecules decompose into hydrogen atoms and spill over to graphene lattice due to the catalysis of Pd.[25,26] A chemical reaction occurs on the surface of Pd-decorated graphene[20]

$$Pd + H_x = PdH_x \quad (3)$$

Since the work function of PdH_x is lower than that of Pd, the formation of PdH_x decreases the transferred amount of electrons from graphene to Pd, which is dependent on the density of H atoms on the graphene.[19,20] The H_2-induced hole density decrease in the Pd/graphene channel is further verified via measuring transfer characteristics of the graphene channel as shown in Figure 4b. The transfer characteristics of the graphene channel were tested at times A, B, and C in Figure 4a through using Si substrate as the back gate. Obviously, the main effect of H_2 is to shift the whole transfer characteristic toward negative V_{gs} direction with negligible shape change, which indicates that

DOI: 10.1021/acsami.5b01070
ACS Appl. Mater. Interfaces 2015, 7, 9581−9588

hydrogen leads to decrease of hole density of the Pd/graphene channel without introducing additional scattering. In previously reported graphene hydrogen sensors, Pd nanoparticles were deposited onto the surface of the whole graphene sample directly,[19,20,27] which resulted in serious problems, such as current leakage, making it difficult to quantitatively describe the transfer characteristics of the graphene channel after Pd decoration. Carrier mobility and transfer characteristics are thus difficult to obtain for analysis.[19,20,27,31−33] In this work, we added an additional EBL process to define the Pd deposition region, which effectively avoids current leakage and paves the way for exploring hydrogen sensing mechanism quantitatively. Experimentally the transconductance of a graphene FET can be obtained from its transfer characteristic using the relation[7]

$$g_m = \frac{\partial I_{ds}}{\partial V_{gs}} = \mu V_{ds} \frac{q}{C_{ox}} \frac{W}{L} \tag{4}$$

in which μ is the carrier mobility, V_{ds} is the voltage bias between the drain and source, q is the electron charge, C_{ox} is the capacitance of the gate oxide, and W/L is the width-to-length ratio of the graphene channel. Since the graphene device here shows approximately linear transfer characteristics, the tranconductance can be estimated as (Figure 4b)

$$\frac{\partial I_{ds}}{\partial V_{gs}} = \frac{\Delta I}{\Delta V} = \frac{I_0 - I_t}{\Delta V} = \frac{V_C}{\Delta V}\left(\frac{1}{R_0} - \frac{1}{R_t}\right) \tag{5}$$

in which ΔI is the current change at zero gate voltage, and ΔV is the horizontal gate voltage shift during hydrogen sensing (marked by green arrows in Figure 4b). The negative shift of the transfer characteristic is caused by the hydrogen-induced hole density decrease, which can be estimated by

$$\Delta V = \frac{\Delta n q}{C_{ox}} \tag{6}$$

where Δn is the hole density change during hydrogen sensing. By combining eqs 4, 5, and 6, R_t can be derived as

$$R_t = \frac{R_0}{1 - k\mu\Delta n} \tag{7}$$

with $k = ((R_0 V_{ds} q^2 W)/(C_{ox}{}^2 V_C L))$ being a constant for a fixed device geometry. Substituting eq 7 into eq 2, the gas response can be written as

$$GR = \frac{k\mu\Delta n}{1 - k\mu\Delta n} \times 100\% \tag{8}$$

Since Δn is small at the beginning of hydrogen sensing, $k\mu\Delta n$ is thus far less than 1.Then eq 8 can be approximated as

$$GR \approx k\mu\Delta n \times 100\% \tag{9}$$

Equation 9 clearly shows that the gas response is dominated by carrier mobility and the hydrogen-induced change in carrier density in the graphene channel. Compared with other materials for H_2 sensing, graphene has higher carrier mobility, which should lead to higher gas response in principle. Furthermore, as indicated by the inset of Figure 4b, ΔV increases linearly with hydrogen response time. Equation 6 then suggests that the change of carrier density Δn also increases linearly with time. Assuming that the rate of hydrogen adsorption and dissociation are constant, the gas response then increases linearly with time as suggested by eq 9, which is consistent with our test results shown in Figure 4a. After 20 min of the recovering process, the transfer characteristic basically coincides with the initial one (Figure 4b), indicating that our graphene sensor is restorable and unharmed during the hydrogen test. It is mentionable that the obtained gas response in this work refers to the percentile resistance change at 10 min. As a matter of fact, the response of our graphene sensors would increase continuously if we extend the response time (Figure S5, Supporting Information).

Figure 4c demonstrates multiple cycles of gas response to 500 ppm hydrogen. The gas responses are found to be between 19.5% and 25%, suggesting that our graphene sensors are highly repeatable and reliable when used for hydrogen sensing. Figure 4d shows the gas response of our graphene sensor to hydrogen concentration ranged from 25 to 1000 ppm, demonstrating the gas response increases with hydrogen concentration. The sensor exhibits a detectable response at ∼2.5% (after 10 min since H_2 on) even at low hydrogen concentration of 25 ppm, and the gas response rises to as high as 32.5% at hydrogen concentration of 1000 ppm. To benchmark the performance of our hydrogen sensor, we compare the gas response of several types of graphene-based hydrogen sensors (Figure 4e).[19,20,27,31−33] The excellent high hydrogen response of our graphene sensors is mainly originated from the high mobility of graphene and well-designed Pd decoration region on the graphene channel. Moreover, our graphene sensors present better linearity on gas response-H_2 concentration relation than other published sensors. Finally the gas response of our sensor is unsaturated with hydrogen concentration even when the concentration reaches 1000 ppm. In contrast, most of the earlier reported graphene hydrogen sensors suffer from gas response saturation at high hydrogen concentration, while the saturation limits the effective measuring range of the sensor.

In addition to the gas response, selectivity is also important for gas sensing. To study the selectivity of our graphene hydrogen sensors, control experiments were conducted to measure the gas response toward 1000 ppm carbon dioxide (CO_2), 1000 ppm methane (CH_4), and 1% oxygen (O_2) (Figure 4f). The response time was also set as 10 min for consistency. CO_2 induced gas response is within 3%, while O_2- and CH_4-induced responses are negligible (within 0.5%). Obviously, our graphene-based sensors are hardly sensitive to these interference gases and can provide excellent selectivity for hydrogen detection.

The two-in-one graphene Hall and hydrogen sensors may in principle provide more powerful functions than either Hall or hydrogen sensors. For example, the multifunctional sensor can be designed as a smart sensor to monitor the concentration and position of hydrogen leakage. Graphene-based sensors work as hydrogen detectors to monitor the dynamic hydrogen concentration. Once hydrogen concentration exceeds a critical value, the resistance of the sensor will increase and pass the target value. Then graphene devices may be switched automatically to Hall sensing mode. Hall devices can be used as position sensors to locate the hydrogen leakage point automatically.[34,35] To implement this idea, a benchmark magnet may be placed at a fixed position. By measuring the output Hall voltage, the magnetic field normal to the Hall sensors can be derived. On the basis of the obtained magnetic field, we can calculate the exact location of graphene device. Consequently, the position of the hydrogen leakage can be determined accurately. More specific descriptions of the application are made in Figure S6 in Supporting Information. Since the combination of magnetic and hydrogen sensing is

DOI: 10.1021/acsami.5b01070
ACS Appl. Mater. Interfaces 2015, 7, 9581−9588

novel, more potential applications may be available in the future.

3. CONCLUSIONS

In conclusion, multifunctional graphene magnetic/hydrogen sensors are constructed for the first time through a simple microfabrication process. The as-fabricated graphene sensor may act as excellent Hall magnetic detector, demonstrating small linearity error within 2% and high magnetic resolution up to 7 $mG/Hz^{0.5}$. Meanwhile the same graphene sensor is also demonstrated as high-performance hydrogen sensor with high gas response, excellent linearity, and great repeatability and selectivity. In particular, the graphene sensor exhibits high hydrogen response up to 32.5% when exposed to 1000 ppm hydrogen, outperforming most graphene-based hydrogen sensors. In addition the hydrogen sensing mechanism of Pd-decorated graphene is systematically explored through investigating its transfer characteristics during gas detection. Our work demonstrates that graphene is a terrific material for multifunctional sensing.

Methods. *Fabrication of Multifunctional Graphene Sensors.* Graphene samples were synthesized on Pt foil following the CVD method, and a bubbling method was utilized to transfer graphene onto the SiO_2 (285 nm)/Si substrate.[36] Before the transfer, the substrate was modified by 3-aminopropyltriethoxysilane to reinforce the adhesion between graphene and the substrate.[7] EBL based on poly(methyl methacrylate) was used to pattern the cross-shaped graphene channel. The redundant graphene was removed by oxygen plasma etching process. The second EBL process was performed to form the electrodes pattern, followed by eletron beam evaporation (EBE, Ti/Au 5/70 nm) and a standard lift-off process in acetone. Another EBL process was utilized to pattern the horizonal channel of graphene sensors. Afterward, 1 nm thickness of Pd nanoparticles was deposited on the graphene sensors by EBE, followed by another lift-off process.

Measurement of Noise. Low-frequency noise of our graphene Hall sensors was measured in accordance with the method we utilized in our previous work.[9] A constant voltage was applied at the horizontal graphene channel; the noise voltage between the vertical electrodes was sent into a low-noise preamplifier SR560. The amplification was set as 100, and the amplified noise signals were acquired through Agilent spectrum analyzer N9020 (Supporting Information, Figure S3).

Gas Detection Test of the Graphene Sensors. The as-fabricated graphene sensors were bonded on a designed printed circuit borad (PCB) through gold wires. The sensors were placed in a sealed chamber with a gas inlet and outlet (Supporting Information, Figure S4). Dupont lines were welded on PCB to connect the graphene sensors and testing system. Hydrogen was diluted with nitrogen, and the concentration was controlled by adjusting the flow rate of the gases. Before turning on testing gas, the sensors were exposed to 750 sccm pure nitrogen for 10 min to stabilize the initial resistance. Hydrogen diluted with nitrogen (750 sccm overall) was then introduced into the chamber to test the dynamic gas response. The response time was set as 10 min; after that time the hydrogen was turned off, and the graphene sensor was let to recover in air. One volt of constant voltage bias was applied at the Pd-decorated graphene channel by Keithley 4200, and dynamic current was measured to characterize the resistance change of the sensor. The sampling time interval was set as 1 s, and all gas sensing tests were performed at room temperature.

ASSOCIATED CONTENT

Supporting Information

Detailed descriptions of the optimization of Pd decoration region and thickness on graphene, noise measurements of graphene Hall sensors, gas-sensing test of graphene hydrogen detectors, and potential application of multifunction sensors. The Supporting Information is available free of charge on the ACS Publications website at DOI: 10.1021/acsami.5b01070.

AUTHOR INFORMATION

Corresponding Authors

*E-mail: zyzhang@pku.edu.cn. (Z.Z.)
*E-mail: lmpeng@pku.edu.cn. (L.-M.P.)

Author Contributions

The manuscript was written through contributions of all authors. Z.Z. and L.M.P. designed the experiment, L.H., Z.L., B.C., X.M., and L.D. performed the growth and transfer of graphene, device fabrication, and characterization. L.H., Z.Z., and L.M.P. analyzed the data and cowrote the manuscript. All authors have given approval to the final version of the manuscript.

Notes

The authors declare no competing financial interest.

ACKNOWLEDGMENTS

This work was supported by the Ministry of Science and Technology of China (Grant Nos. 2011CB933001 and 2011CB933002), National Science Foundation of China (Grant Nos. 61322105, 61321001, and 61390504). We sincerely appreciate Prof. C. Qing from Dept. of Electronics in Peking Univ. for providing the gas-sensing equipment for our experiment.

REFERENCES

(1) Grober, V.; Heydenbluth, D.; Moos, R.; Rein, D.; Sauerer, J.; Simmons, T.; Sinn, W.; Werthschutzky, R.; Wilde, J. *Sensor Trends 2014;* AMA Association for Sensor Technology: Berlin, Germany, 2010.

(2) Novoselov, K. S.; FalKo, V. I.; Colombo, L.; Gellert, P. R.; Schwab, M. G.; Kim, K. A Roadmap for Graphene. *Nature* **2012**, *490*, 192−200.

(3) Hill, E. W.; Vijayaragahvan, A.; Novoselov, K. S. Graphene Sensors. *IEEE Sens. J.* **2011**, *11*, 3161−3170.

(4) He, Q.; Wu, S.; Yin, Z.; Zhang, H. Graphene-based Electronic Sensors. *Chem. Sci.* **2012**, *3*, 1764−1772.

(5) Huang, L.; Zhang, Z.; Chen, B.; Ma, X.; Zhong, H.; Peng, L.-M. Ultra-sensitive Graphene Hall Elements. *Appl. Phys. Lett.* **2014**, *104*, 183106.

(6) Xu, H.; Zhang, Z.; Shi, R.; Liu, H.; Wang, Z.; Wang, S.; Peng, L.-M. Batch-Fabricated High-Performance Graphene Hall Elements. *Sci. Rep.* **2013**, *3*, 1207.

(7) Shi, R.; Xu, H.; Chen, B.; Zhang, Z.; Peng, L.-M. Scalable Fabrication of Graphene Devices through Photolithography. *Appl. Phys. Lett.* **2013**, *102*, 113102.

(8) Huang, L.; Xu, H.; Zhang, Z.; Chen, C.; Jiang, J.; Ma, X.; Chen, B.; Li, Z.; Zhong, H.; Peng, L.-M. Graphene/Si CMOS Hybrid Hall Integrated Circuits. *Sci. Rep.* **2014**, *4*, 5548.

(9) Xu, H.; Huang, L.; Zhang, Z.; Chen, B.; Zhong, H.; Peng, L.-M. Flicker Noise and Magnetic Resolution of Graphene Hall Sensors at Low Frequency. *Appl. Phys. Lett.* **2013**, *103*, 112405.

(10) Chiu-Chun, T.; Ming-Yang, L.; Li, L. J.; Chi, C. C.; Chen, J. C. Characteristics of a Sensitive Micro-Hall Probe Fabricated On Chemical Vapor Deposited Graphene Over the Temperature Range From Liquid-Helium to Room Temperature. *Appl. Phys. Lett.* **2011**, *99*, 112107.

DOI: 10.1021/acsami.5b01070
ACS Appl. Mater. Interfaces 2015, 7, 9581−9588

(11) Rajkumar, R. K.; Asenjo, A.; Panchal, V.; Manzin, A.; Iglesias-Freire, O.; Kazakova, O. Magnetic scanning gate microscopy of graphene Hall devices (invited). *J. Appl. Phys.* **2014**, *115*, 172606.
(12) Sonusen, S.; Karci, O.; Dede, M.; Aksoy, S.; Oral, A. Single layer graphene Hall sensors for scanning Hall probe microscopy(SHPM) in 3−300 K temperature range. *Appl. Surf. Sci.* **2014**, *308*, 414−418.
(13) Schedin, F.; Geim, A. K.; Morozov, S. V.; Hill, E. W.; Blake, P.; Katsnelson, M. I.; Novoselov, K. S. Detection of Individual Gas Molecules Adsorbed on Graphene. *Nat. Mater.* **2007**, *6*, 652−655.
(14) Gautam, M.; Jayatissa, A. H. Gas Sensing Properties of Graphene Synthesized by Chemical Vapor Deposition. *Mater. Sci. Eng., C* **2011**, *31*, 1405−1411.
(15) Furchi, M.; Urich, A.; Pospischil, A.; Lilley, G.; Unterrainer, K.; Detz, H.; Klang, P.; Andrews, A. M.; Schrenk, W.; Strasser, G.; Mueller, T. Microcavity-Integrated Graphene Photodetector. *Nano Lett.* **2012**, *12*, 2773−2777.
(16) Smith, A. D.; Vaziri, S.; Niklaus, F.; Fischer, A. C.; Sterner, M.; Delin, A.; Ostling, M.; Lemme, M. C. Pressure Sensors based on Suspended Graphene Membranes. *Solid-State Electron.* **2013**, *88*, 89−94.
(17) Park, S. J.; Kwon, O. S.; Lee, S. H.; Song, H. S.; Park, T. H.; Jang, J. Ultrasensitive Flexible Graphene Based Field-Effect Transistor (FET)-Type Bioelectronic Nose. *Nano Lett.* **2012**, *12*, 5082−5090.
(18) Ohno, Y.; Maehashi, K.; Yamashiro, Y.; Matsumoto, K. Electrolyte-Gated Graphene Field-Effect Transistors for Detecting pH and Protein Adsorption. *Nano Lett.* **2009**, *9*, 3318−3822.
(19) Chung, M. G.; Kim, D.; Seo, D. K.; Kim, T.; Im, H. U.; Lee, H. M.; Yoo, J.; Hong, S.; Kang, T. J.; Kim, Y. H. Flexible Hydrogen Sensors using Graphene with Palladium Nanoparticle Decoration. *Sens. Actuators, B* **2012**, *169*, 387−392.
(20) Wu, W.; Liu, Z.; Jauregui, L. A.; Yu, Q.; Pillai, R.; Cao, H.; Bao, J.; Chen, Y. P.; Pei, S. Wafer-scale Synthesis of Graphene by Chemical Vapor Deposition and its Application in Hydrogen Sensing. *Sens. Actuators, B* **2010**, *150*, 296−300.
(21) Popovic, R. S. *Hall Effect Devices;* Institute of Physics Publishing: Philadelphia, PA, 2004.
(22) Lu, C.; Chen, Z. High-Temperature Resistive Hydrogen Sensor based on Thin Nanoporous Rutile TiO2 Film on Anodic Aluminum Oxide. *Sens. Actuators, B* **2009**, *140*, 109−115.
(23) Varghese, O. K.; Gong, D. W.; Paulose, M.; Ong, K. G.; Grimes, C. A. Hydrogen Sensing using Titania Nanotubes. *Sens. Actuators., B* **2003**, *93*, 338−344.
(24) Ma, L.; Wu, Z.; Li, J.; Wu, E.; Ren, W.; Cheng, H. Hydrogen Adsorption Behavior of Graphene above Critical Temperature. *Int. J. Hydrogen Energy* **2009**, *34*, 2329−2332.
(25) Lopez-Corral, I.; German, E.; Juan, A.; Volpe, M. A.; Brizuela, G. P. DFT Study of Hydrogen Adsorption on Palladium Decorated Graphene. *J. Phys. Chem. C* **2011**, *115*, 4315−4323.
(26) Lopez-Corral, I.; German, E.; Juan, A.; Volpe, M. A.; Brizuela, G. P. Hydrogen Adsorption on Palladium Dimer Decorated Graphene: A Bonding Study. *Int. J. Hydrogen Energy* **2012**, *37*, 6653−6665.
(27) Pak, Y.; Kim, S.; Jeong, H.; Kang, C. G.; Park, J. S.; Song, H.; Lee, R.; Myoung, N.; Lee, B. H.; Seo, S.; Kim, J. T.; Jung, G. Palladium-Decorated Hydrogen-Gas Sensors Using Periodically Aligned Graphene Nanoribbons. *ACS Appl. Mater. Interfaces* **2014**, *6*, 13293−13298.
(28) Sun, Y.; Wang, H. H. High-Performance, Flexible Hydrogen Sensors That Use Carbon Nanotubes Decorated with Palladium Nanoparticles. *Adv. Mater.* **2007**, *19*, 2818−2823.
(29) Kolmakov, A.; Klenov, D. O.; Lilach, Y.; Stemmer, S.; Moskovits, M. Enhanced Gas Sensing by Individual SnO2 Nanowires and Nanobelts Functionalized with Pd Catalyst Particles. *Nano Lett.* **2005**, *5*, 667−673.
(30) Johnson, J. L.; Behnam, A.; Pearton, S. J.; Ural, A. Hydrogen Sensing Using Pd-Functionalized Multi-Layer Graphene Nanoribbon Networks. *Adv. Mater.* **2010**, *22*, 4877−4880.
(31) Al-Mashat, L.; Shin, K.; Kalantar-zadeh, K.; Plessis, J. D.; Han, S. H.; Kojima, R. W.; Kaner, R. B.; Li, D.; Gou, X.; Ippolito, S. J.; Wlodarski, W. Graphene/Polyaniline Nanocomposite for Hydrogen Sensing. *J. Phys. Chem. C* **2010**, *114*, 16168−16173.
(32) Chu, B. H.; Nicolosi, J.; Lo, C. F.; Strupinski, W.; Pearton, S. J.; Ren, F. Effect of Coated Platinum Thickness on Hydrogen Detection Sensitivity of Graphene-Based Sensors. *Electrochem. Solid-State Lett.* **2011**, *14*, K43−K45.
(33) Kim, K.; Lee, H.; Johnson, R. W.; Tanskanen, J. T.; Liu, N.; Kim, M.; Pang, C.; Ahn, C.; Bent, S. F.; Bao, Z. Selective Metal Deposition at Graphene Line Defects by Atomic Layer Deposition. *Nat. Commun.* **2014**, *5*, 4781.
(34) Schlageter, V.; Besse, P. A.; Popovic, R. S.; Kucera, P. Tracking System with Five Deagrees of Freedom using a 2D-array of Hall Sensors and a Permanent Magnet. *Sens. Actuators, A* **2001**, *92*, 37−42.
(35) Burger, F.; Besse, P. A.; Popovic, R. S. New fully Integrated 3-D Siliocn Hall Sensor for Precise Angular-Position Measurements. *Sens. Actuators, A* **1998**, *67*, 72−76.
(36) Gao, L.; Ren, W.; Xu, H.; Jin, L.; Wang, Z.; Ma, T.; Ma, L.; Zhang, Z.; Fu, Q.; Peng, L.-M.; Bao, X.; Cheng, H. Repeated Growth and Bubbling Transfer of Graphene with Millimetre-size Single-crystal Grains using Platinum. *Nat. Commun.* **2012**, *3*, 699.

DOI: 10.1021/acsami.5b01070
ACS Appl. Mater. Interfaces 2015, 7, 9581−9588